

Mechanism and Driving Force of NO Transfer from S-Nitrosothiol to Cobalt(II) Porphyrin: A Detailed Thermodynamic and Kinetic Study

Xiao-Qing Zhu,* Jian-Yu Zhang, and Jin-Pei Cheng*

Department of Chemistry and the State Key Laboratory of Elemento-Organic Chemistry, Nankai University, Tianjin 300071, China

Received July 29, 2006

The thermodynamics and kinetics of NO transfer from S-nitrosotriphenylmethanethiol (Ph_3CSNO) to a series of $\alpha,\beta,\gamma,\delta$ -tetraphenylporphinatocobalt(II) derivatives $[\text{T}(\text{G})\text{PPCo}^{\text{II}}]$, generating the nitrosyl cobalt atom center adducts $[\text{T}(\text{G})\text{PPCo}^{\text{II}}\text{NO}]$, in benzonitrile were investigated using titration calorimetry and stopped-flow UV-vis spectrophotometry, respectively. The estimation of the energy change for each elementary step in the possible NO transfer pathways suggests that the most likely route is a concerted process of the homolytic S–NO bond dissociation and the formation of the Co–NO bond. The kinetic investigation on the NO transfer shows that the second-order rate constants at room temperature cover the range from 0.76×10^4 to $4.58 \times 10^4 \text{ M}^{-1} \text{ s}^{-1}$, and the reaction rate was mainly governed by activation enthalpy. Hammett-type linear free-energy analysis indicates that the NO moiety in Ph_3CSNO is a Lewis acid and the $\text{T}(\text{G})\text{PPCo}^{\text{II}}$ is a Lewis base; the main driving force for the NO transfer is electrostatic charge attraction rather than the spin–spin coupling interaction. The effective charge distribution on the cobalt atom in the cobalt porphyrin at the various stages, the reactant $[\text{T}(\text{G})\text{PPCo}^{\text{II}}]$, the transition-state, and the product $[\text{T}(\text{G})\text{PPCo}^{\text{II}}\text{NO}]$, was estimated to show that the cobalt atom carries relative effective positive charges of 2.000 in the reactant $[\text{T}(\text{G})\text{PPCo}^{\text{II}}]$, 2.350 in the transition state, and 2.503 in the product $[\text{T}(\text{G})\text{PPCo}^{\text{II}}\text{NO}]$, which indicates that the concerted NO transfer from Ph_3CSNO to $\text{T}(\text{G})\text{PPCo}^{\text{II}}$ with the release of the $\text{Ph}_3\text{CS}^{\bullet}$ radical was actually performed by the initial negative charge (-0.350) transfer from $\text{T}(\text{G})\text{PPCo}^{\text{II}}$ to Ph_3CSNO to form the transition state and was followed by homolytic S–NO bond dissociation of Ph_3CSNO with a further negative charge (-0.153) transfer from $\text{T}(\text{G})\text{PPCo}^{\text{II}}$ to the NO group to form the final product $\text{T}(\text{G})\text{PPCo}^{\text{II}}\text{NO}$. It is evident that these important thermodynamic and kinetic results would be helpful in understanding the nature of the interaction between RSNO and metal porphyrins in both chemical and biochemical systems.

Introduction

Extensive research into nitric oxide (NO) has been stimulated since the discovery that NO plays essential regulatory roles in processes such as smooth-muscle relaxation, regulation of blood pressure, modulation of neurotransmission, and platelet adhesion in vivo.¹ A number of disease states involving NO imbalances were proposed, and much attention has been given to the chemistry, biology, and pharmacology of NO and the compounds which can

directly react with it.² Since the metal centers are generally regarded as the principal targets for NO in mammalian biology, the interaction of free NO with metal complexes such as metal porphyrins is of special interest, and this area has been studied extensively.^{3–11} However, a great deal of

* To whom correspondence should be addressed. E-mail: xqzhu@nankai.edu.cn (X.-Q.Z.).

(1) (a) Feldman, P. L.; Griffith, O. W.; Stuehr, D. J. *Chem. Eng. News* **1993**, 71, 26. (b) Karupiah, G.; Xie, Q.; Buller, R. M. L.; Nathan, C.; Duarte, C.; MacMicking, J. D. *Science* **1993**, 261, 1445. (c) Lipton, S. L. *Nature* **1993**, 364, 626. (d) Edelman, G. M.; Gally, J. A. *Proc. Natl. Acad. Sci. U.S.A.* **1992**, 89, 11651.

(2) (a) Palmer, R. M. J.; Ferrige, A. G.; Moncada, S. *Nature* **1987**, 327, 524–526. (b) Hibbs, J. B., Jr.; Taintor, R. R.; Vavrin, Z. *Science* **1987**, 235, 473–476. (c) Moncada, S.; Palmer, R. M. J.; Higgs, E. A. *Pharmacol. Rev.* **1991**, 43, 109–142. (d) Wink, D. A.; Hanbauer, I.; Grisham, M. B.; Laval, F.; Nims, R. W.; Laval, J.; Cook, J.; Pacelli, R.; Liebmann, J.; Krishna, M.; Ford, P. C.; Mitchell, J. B. *Curr. Top. Cell. Regul.* **1996**, 34, 159–187. (3) (a) Coppens, P.; Novozhilova, I.; Kovalevsky, A. *Chem. Rev.* **2002**, 102, 861–883. (b) Ford, P. C.; Lorkovic, I. M. *Chem. Rev.* **2002**, 102, 993–1017. (c) Butler, A. R.; Megson, I. L. *Chem. Rev.* **2002**, 102, 1155–1165. (d) Wasser, I. M.; de Vries, S.; Moenne-Loccoz, P.; Schroder, I.; Karlin, K. D. *Chem. Rev.* **2002**, 102, 1201–1234. (4) Richter-Addo, G. B. *Acc. Chem. Res.* **1999**, 32, 529–536 and references therein.

evidence has shown that the concentration of free NO in mammalian tissue is very low (~4 nM); the species most related to NO found in mammalian tissue are nitrate, nitrite, and NO-donors,^{12,13} which means that the interaction of metal center complexes such as metal porphyrin with NO-donors may be more common and important than that with free NO in vivo.¹⁴ Since S-nitrosothiols (RSNOs) show many important biological properties similar to those of NO itself and generally have been regarded as the best candidates for the endogenous storage and transports of NO^{13,15–17} and metal porphyrins have been regarded as the most likely target to accept NO in vivo, the interaction of RSNOs with metal porphyrins should be not only very important but also ubiquitous in vivo.^{3,6,13} However, bibliographic research shows that compared to the reports on the interaction of free NO with metal porphyrin, the publication with respect to the interaction of RSNOs with metal porphyrin is quite poor, and the many important chemical questions for this aspect are still not clear.^{13,18} What are the final products of the reaction of RSNOs with metal porphyrin? What is the form of NO in the initial transfer step from RSNOs to metal porphyrin? Is it NO⁺, NO, or NO[–]? What are the energy

Table 1. Enthalpy Changes of the Reactions of Ph₃CSNO with T(G)PPCo^{II} in Benzonitrile (kcal/mol) along with Redox Potentials of T(G)PPCo^{II} and T(G)PPCo^{II}NO in Benzonitrile (V vs Fc)

substituents (G)	ΔH_r^a	$E_{1/2}[\text{T(G)PPCo}^{\text{II}}\text{NO}]^b$	$E_{1/2}[\text{T(G)PPCo}^{\text{II}}]^b$
<i>p</i> -OMe	–31.6	0.887	0.581
<i>p</i> -Me	–31.1	0.923	0.621
<i>p</i> -i-pr	–31.0	0.925	0.608
<i>m</i> -Me	–30.6	0.945	0.646
<i>p</i> -H	–30.2	0.962	0.676
<i>m</i> -OMe	–29.9	0.967	0.684
<i>p</i> -Cl	–29.4	1.014	0.731
<i>p</i> -Br	–29.5	1.015	0.733
<i>m</i> -Cl	–29.6	1.055	0.772
<i>m</i> -Br	–29.3	1.058	0.775
<i>m</i> -NO ₂	–27.8	1.105	0.844
<i>p</i> -NO ₂	–27.6	1.131	0.872

^a Measured in benzonitrile at 298 K in kcal/mol by titration calorimetry. The data given were the average values of at least two independent runs, each of which was again an average value of at least 9 consecutive titrations. The reproducibility was ≤ 1.0 kcal/mol. ^b Measured in benzonitrile at 298 K in V, taken as first redox potentials by CV method vs the ferrocenium/ferrocene redox couple. Reproducible to 5 mV or better.

changes of each elementary step in the pathway of the NO transfer from RSNOs to metal porphyrin? What are the kinetic characters of the NO transfer from RSNOs to metal porphyrin in the rate-determining step? What is the nature of the driving force which pushes NO transfer from RSNOs to metal porphyrin? Is it the electrostatic dipole charge attraction or the spin–spin coupling interaction? It is evident that all these interesting questions should be the keys to open the door of comprehensively understanding the interaction mechanism of metal porphyrins with RSNOs. In the present article, S-nitrosotriphenylmethanethiol (Ph₃CSNO) was chosen as representative of S-nitrosothiols, and tetraphenylporphinatocobalt(II) derivatives [T(G)PPCo^{II}] were chosen as the model of metal porphyrins.¹⁹ Detailed thermodynamics and kinetics of the NO transfer from Ph₃CSNO to a series of T(G)PPCo^{II} in benzonitrile were investigated using titration calorimetry and stopped-flow spectrophotometry, respectively. The experimental results can be used to answer the above-mentioned questions.

Results

Twelve para- and meta-substituted $\alpha,\beta,\gamma,\delta$ -tetraphenylporphinatocobalts(II) [T(G)PPCo^{II}] were synthesized according to the literature method^{19a,20} and were treated with S-nitrosotriphenylmethanethiol (Ph₃CSNO) in benzonitrile at room temperature to give the corresponding cobalt-nitrosyl product para- or meta-substituted nitrosyl- $\alpha,\beta,\gamma,\delta$ -tetraphenylporphinatocobalt(II) [T(G)PPCo^{II}NO] and the dimer trityldisulfide (Ph₃CS)₂ as the final products without any coordination of RSNO to the Co center porphyrin (eq 1).²¹ The products were identified by MS, ¹H NMR, and UV–vis spectra. The stoichiometry of reaction 1 was obtained

- (5) (a) Suzuki, N.; Higuchi, T.; Urano, Y.; Kikuchi, K.; Uchida, T.; Mukai, M.; Kitagawa, T.; Nagano, T. *J. Am. Chem. Soc.* **2000**, *122*, 12059–12060. (c) Linder, D. P.; Rodgers, K. R.; Banister, J.; Wyllie, G. R. A.; Ellison, M. K.; Scheidt, W. R. *J. Am. Chem. Soc.* **2004**, *126*, 14136–14148.
- (6) (a) Hoshino, M.; Laverman, L.; Ford, P. C. *Coord. Chem. Rev.* **1999**, *187*, 75–102 and references therein. (b) Laverman, L.; Ford, P. C. *Coord. Chem. Rev.* **2005**, *249*, 391–403 and references therein.
- (7) Lim, M. D.; Lorkovic, I. M.; Ford, P. C. *J. Inorg. Biochem.* **2005**, *99*, 151–165 and references therein.
- (8) (a) Hoshino, M.; Kogure, M. *J. Phys. Chem.* **1989**, *93*, 5478. (b) Morlino, E. A.; Rodgers, M. A. J. *J. Am. Chem. Soc.* **1996**, *118*, 11798–11804. (c) Hoshino, M.; Nagashima, Y.; Seki, H. *Inorg. Chem.* **1998**, *37*, 2464–2469.
- (9) (a) Wolak, M.; Stochel, G.; Hamza, M.; van Eldik, R. *Inorg. Chem.* **2000**, *39*, 2018. (b) Zheng, D.; Birke, R. L. *J. Am. Chem. Soc.* **2001**, *123*, 4637.
- (10) (a) Thamae, M. A.; Nyokong, T. *J. Porphyrins Phthalocyanines* **2001**, *5*, 839–845. (b) Wolak, M.; Zahl, A.; Schnepfensieper, T.; Stochel, G.; van Eldik, R. *J. Am. Chem. Soc.* **2001**, *123*, 9780–9791. (c) Zheng, D.; Birke, R. L. *J. Am. Chem. Soc.* **2002**, *124*, 9066–9067. (d) Sharma, V. S.; Pilz, R. B.; Boss, G. R.; Magde, D. *Biochemistry* **2003**, *42*, 8900–8908.
- (11) (a) Hoshino, M.; Ozawa, K.; Seki, H.; Ford, P. C. *J. Am. Chem. Soc.* **1993**, *115*, 9568–9575. (b) Laverman, L. E.; Hoshino, M.; Ford, P. C. *J. Am. Chem. Soc.* **1997**, *119*, 12663–12664. (c) Laverman, L. E.; Ford, P. C. *J. Am. Chem. Soc.* **2001**, *123*, 11614–11622. (d) Kurtikyan, T. S.; Martirosyan, G. G.; Lorkovic, I. M.; Ford, P. C. *J. Am. Chem. Soc.* **2002**, *124*, 10124–10129. (e) Fernandez, B. O.; Lorkovic, I. M.; Ford, P. C. *Inorg. Chem.* **2004**, *43*, 5393–5402. (f) Kurtikyan, T. S.; Gulyan, G. M.; Martirosyan, G. G.; Lim, M. D.; Ford, P. C. *J. Am. Chem. Soc.* **2005**, *127*, 6216–6224.
- (12) Bellamy, T. C.; Griffiths, C.; Garthwaite, J. *J. Biol. Chem.* **2002**, *277*, 31801–31807.
- (13) Wang, P. G.; Xian, M.; Tang, X.-P.; Wu, X.-J.; Wen, Z.; Cai, T.-W.; Janczuk, A. J. *Chem. Rev.* **2002**, *102*, 1091–1134.
- (14) Zhang, Y.; Hogg, N. *Free Radical Biol. Med.* **2004**, *36*, 947.
- (15) Williams, D. L. H. *Acc. Chem. Res.* **1999**, *32*, 869–876 and references therein.
- (16) Malinski, T.; Bailey, F.; Zhang, Z. G.; Chopp, M. *J. Cereb. Blood Flow Metab.* **1993**, *13*, 355–358.
- (17) (a) Andreassen, L. V.; Lorkovic, I. M.; Richter-Addo, G. B.; Ford, P. C. *Nitric Oxide: Biol. Chem.* **2002**, *6*, 228–235. (b) Lee, J.; Chen, L.; West, A. H.; Richter-Addo, G. B. *Chem. Rev.* **2002**, *102*, 1019–1065.
- (18) (a) de Oliveira, M. G.; Shishido, S. M.; Seabra, A. B.; Morgon, N. H. *J. Phys. Chem. A*, **2002**, *106*, 8963–8970 and references therein. (b) Anthony, R. B.; Peter, R. *Anal. Biochem.* **1997**, *249*, 1–9. (c) Zhu, X.-Q.; Zhang, J.-Y.; Mei, L.-R.; Cheng, J.-P. *Org. Lett.* **2006**, *8*, 3065–3067.
- (19) (a) Zhu, X.-Q.; Li, Q.; Hao, W.-F.; Cheng, J.-P. *J. Am. Chem. Soc.* **2002**, *124*, 9887–9893 and references therein. (b) Zhu, X.-Q.; Hao, W.-F.; Tang, H.; Wang, C.-H.; Cheng, J.-P. *J. Am. Chem. Soc.* **2005**, *127*, 2696–2708.
- (20) Alder, A. D.; Longo, F. R.; Finarelli, J. D.; Goldmacher, J.; Assour, J.; Korsakoff, L. *J. Org. Chem.* **1967**, *32*, 476.
- (21) The combination of Ph₃CSNO and T(G)PPCo^{II} may occurred before the NO initial transfer, while the RSNO–Co porphyrin coordinated product wasn't obtained.

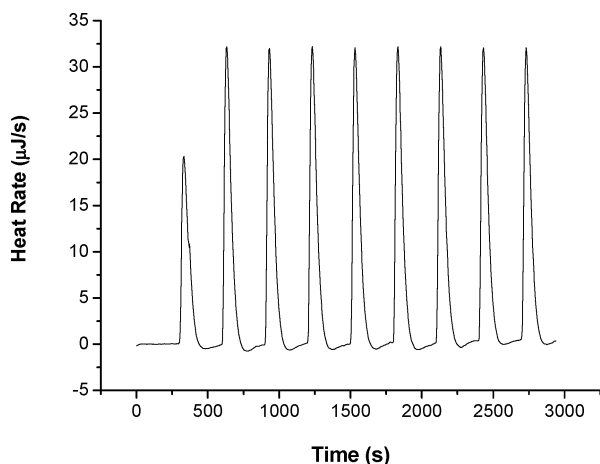
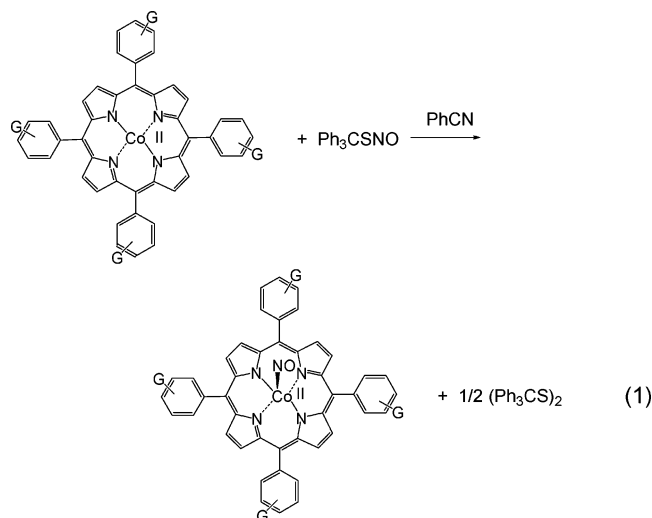


Figure 1. Isothermal titration calorimetry (ITC) for the reaction heat of Ph_3CSNO with $\text{T(H)PPCo}^{\text{II}}$ in benzonitrile at 298 K. Titration was conducted by adding $10\ \mu\text{L}$ of $\text{T(H)PPCo}^{\text{II}}$ (1.8 mM) every 300 s into the benzonitrile containing Ph_3CSNO ($\sim 1.2\ \text{mM}$).

from the product analyses via the reaction of various molar ratios of Ph_3CSNO and $\text{T(G)PPCo}^{\text{II}}$. The results suggest that 1 mol of $\text{T(G)PPCo}^{\text{II}}$ is required to consume 1 mol of Ph_3CSNO thoroughly to form 1 mol of $\text{T(G)PPCo}^{\text{II}}\text{NO}$ and 0.5 mol of trityldisulfide (Figure S1 in Supporting Information). The reaction heats were determined with titration calorimetry (Figure 1), and the redox potentials of the relative species were measured using the CV method.^{19a} Detailed experimental results are summarized in Table 1.



The kinetics of reaction 1 were monitored at different wavelengths (from 415 to 420 nm) depending on the substituents of $\text{T(G)PPCo}^{\text{II}}$ using stopped-flow spectrometry under pseudo-first-order conditions with Ph_3CSNO in more than 15-fold excess (Figure 2). The decays of $\text{T(G)PPCo}^{\text{II}}$ absorbance followed single exponentials from which pseudo-first-order rate constants were derived. The second-order rate constants, k_2 , at different temperatures between 298 and 318 K are given in Table 2, which were derived from the line slope of the plots of the pseudo-first-order rate constants versus the concentrations of Ph_3CSNO (Figure S7 in Supporting Information). The Arrhenius activation energy (ΔE_a) and Eyring activation parameters: activation enthalpy (ΔH^\ddagger)

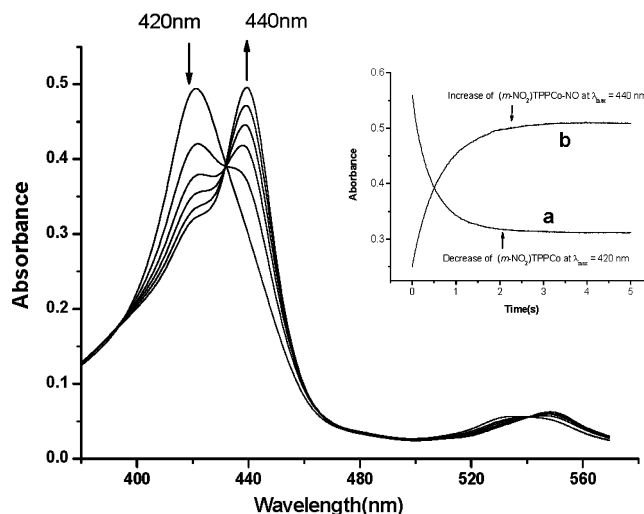


Figure 2. UV-vis spectra obtained from the reaction of Ph_3CSNO ($[\text{Ph}_3\text{CSNO}] = 5.63 \times 10^{-4}\ \text{M}$) with $(m\text{-NO}_2)\text{Co}^{\text{II}}\text{TPP}$ ($[(m\text{-NO}_2)\text{Co}^{\text{II}}\text{TPP}] = 6.33 \times 10^{-5}\ \text{M}$) in benzonitrile at $25\ ^\circ\text{C}$ at time intervals of 125, 375, 625, 875, 1250, and 1875 ms (going down). The inset shows the (a) decay of the kinetic trace for $\text{T}(m\text{-NO}_2)\text{PPCo}^{\text{II}}$ monitored at 420 nm and the (b) growth of the kinetic trace for $\text{T}(m\text{-NO}_2)\text{PPCo}^{\text{II}}\text{NO}$ monitored at 440 nm.

Table 2. Second-Order Rate Constants, k_2 , for the Reactions of Ph_3CSNO with $\text{T(G)PPCo}^{\text{II}}$ in Benzonitrile at Different Temperatures between 298 and 318 K^a

G	$k_2 (\times 10^{-3}\ \text{M}^{-1}\ \text{s}^{-1})$				
	298 K	303 K	308 K	313 K	318 K
<i>p</i> -OCH ₃	45.80	61.95	77.05	100.45	125.10
<i>p</i> -CH ₃	40.90	53.18	67.27	89.21	114.25
<i>p</i> -i-pr	34.57	46.68	60.83	77.58	96.03
<i>m</i> -CH ₃	32.84	43.44	56.14	74.80	91.52
<i>p</i> -H	30.88	41.40	53.74	69.34	84.00
<i>m</i> -OCH ₃	24.98	32.20	42.30	56.52	70.28
<i>p</i> -Cl	19.18	25.12	35.10	46.76	58.14
<i>p</i> -Br	18.78	24.85	34.42	45.41	57.25
<i>m</i> -Cl	16.30	22.48	28.58	39.12	48.58
<i>m</i> -Br	15.72	21.34	28.18	37.58	48.68
<i>m</i> -NO ₂	7.74	10.57	14.24	19.47	26.45
<i>p</i> -NO ₂	7.55	10.36	14.20	19.58	25.96

^a Standard deviation of $< 5\%$.

and activation entropy (ΔS^\ddagger) for the reaction of Ph_3CSNO with $\text{T(G)PPCo}^{\text{II}}$ in benzonitrile are summarized in Table 3; they were derived from Arrhenius plots of $\ln k_2$ and Eyring plots of $\ln(k_2/T)$ versus the reciprocal of the absolute temperature ($1/T$), respectively (Figures S8–S13 in Supporting Information). The heterolytic S–NO bond dissociation energy of Ph_3CSNO in benzonitrile [$\Delta H_{\text{het}}(\text{S–NO})$] was obtained from the reaction heat of the triphenylmethanethiol anion (Ph_3CS^-) with NO^+ cation ($\text{NO}^+\text{ClO}_4^-$) in dry anaerobic benzonitrile solution (see experimental details in Supporting Information); the result is given in Table 4^{22–23}. The homolytic S–NO bond dissociation energy of Ph_3CSNO [$\Delta H_{\text{homo}}(\text{S–NO})$], as well as the heterolytic and homolytic ($\text{S–NO})^\bullet$ bond dissociation energies for the radical anion

(22) The S–S BDE of $(\text{Ph}_3\text{CS})_2$ (60.4 kcal/mol) is smaller than that of S_8 (63.6 kcal/mol) by ~ 3.2 kcal/mol, the reason could be the steric hindrance of the former being larger than that of the latter. (cf., Brown, T. L.; LeMay, H. E. Jr.; Bursten, B. E. *Chemistry the Central Science*; Pearson Education North Asia Limited and China Machine Press, Prentice Hall Inc.: Shanghai, China, 2002; p 289).

(23) Wayner, D. D. M.; Parker, V. D. *Acc. Chem. Res.* **1993**, 26, 287–294.

Table 3. Activation Parameters for the Reactions of Ph₃CSNO with T(G)PPCo^{II} in Benzonitrile

G	ΔE_a^a	ΔH^\ddagger^b	ΔS^\ddagger^c	$-T\Delta S^\ddagger^d$	ΔG^\ddagger^e
<i>p</i> -OCH ₃	9.4	8.8	-7.75	2.3	11.1
<i>p</i> -CH ₃	9.7	9.1	-7.05	2.1	11.2
<i>p</i> -i-pr	9.6	9.0	-7.55	2.3	11.3
<i>m</i> -CH ₃	9.8	9.2	-7.16	2.1	11.3
<i>p</i> -H	9.5	8.9	-8.20	2.4	11.3
<i>m</i> -OCH ₃	9.9	9.3	-7.26	2.2	11.5
<i>p</i> -Cl	10.7	10.1	-5.13	1.5	11.6
<i>p</i> -Br	10.7	10.1	-5.26	1.6	11.7
<i>m</i> -Cl	10.3	9.7	-6.71	2.0	11.7
<i>m</i> -Br	10.7	10.0	-5.69	1.7	11.7
<i>m</i> -NO ₂	11.6	11.0	-4.08	1.2	12.2
<i>p</i> -NO ₂	11.7	11.1	-3.63	1.1	12.2

^a From the slope of the Arrhenius plots; the units are kcal/mol. ^b From the slope of the Eyring plots; the units are kcal/mol. ^c From the intercept of the Eyring plots; the units are cal mol⁻¹ K⁻¹. ^d The units are kcal/mol and *T* = 298 K. ^e Obtained from the equation $\Delta G^\ddagger = \Delta H^\ddagger - T\Delta S^\ddagger$; the units are kcal/mol.

Table 4. Enthalpy Change of the Reaction of Ph₃CS⁻ with the NO⁺ Cation, Dissociation Energies of the Heterolytic and Homolytic S–NO Bond of Ph₃CSNO and Its Radical Anion, Dissociation Energy of the Homolytic S–S Bond of Ph₃CS–SCPh₃, and Redox Potentials of the Relative Species in Benzonitrile

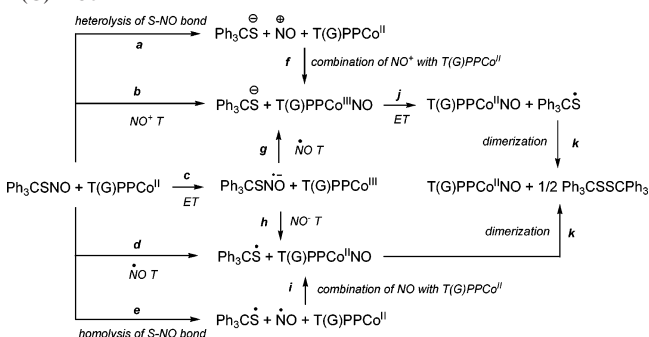
ΔH_f	-52.1 ^a	$\Delta H_{het}(\text{Ph}_3\text{CS}-\text{NO})$	52.1 ^d
$E_{1/2}(\text{NO}^{+/0})$	0.8265 ^b	$\Delta H_{homo}(\text{Ph}_3\text{CS}-\text{NO})$	23.4 ^e
$E_{1/2}(\text{NO}^{0/-})$	-0.287 ^b	$\Delta H_{het}(\text{S}-\text{NO})^{\cdot-}$	3.4 ^f
$E_{red}^{\circ}(\text{Ph}_3\text{CSNO}^{0/-})$	-1.156 ^c	$\Delta H_{homo}(\text{S}-\text{NO})^{\cdot-}$	7.4 ^g
$E_{ox}^{\circ}(\text{Ph}_3\text{CSNO}^{+/0})$	1.704 ^c	$\Delta H_{homo}(\text{S}-\text{S})$	60.4 ^{h,22}
$E_{ox}^{\circ}(\text{Ph}_3\text{CS}^{0/-})$	-0.418 ^c		

^a ΔH_f is the enthalpy change of the reaction of NO⁺ with anion Ph₃CS⁻, derived from the reaction heat of NO⁺ with Ph₃CS⁻ in benzonitrile by switching the sign of the heat value, which was determined by using isothermal titration calorimetry (ITC); the reproducibility was within 1.0 kcal/mol, and the units are kcal/mol. ^b Measured at 298 K in V vs Fc by CV. Reproducible to 10 mV or better. ^c The standard redox potentials were derived from the corresponding irreversible redox potentials calibrated by using Wayner and Parker's method²³ respectively; the units are V vs Fc. ^d Derived from the enthalpy change of the reaction of NO⁺ with Ph₃CS⁻ in benzonitrile; the units are kcal/mol. ^e Obtained from the equation S3; the units are kcal/mol. ^f Obtained from the equation S4; the uncertainty is estimated to be ≤ 1 kcal/mol, and the units are kcal/mol. ^g Obtained from equation S5; the uncertainty is estimated to be ≤ 1 kcal/mol, and the units are kcal/mol. ^h Derived from the reaction heat of Ph₃CSNO with T(H)PPCo^{II}, according to the equation $\Delta H_{homo}(\text{S}-\text{S}) = 2\Delta H_{homo}(\text{S}-\text{NO}) - 2\Delta H_{homo}(\text{Co}^{II}-\text{NO}) - 2\Delta H_{rxn}$; the uncertainty is estimated to be ≤ 2 kcal/mol, and the units are kcal/mol.

of Ph₃CSNO, was also estimated according to the equations S3–S5, which were derived from appropriate thermodynamic cycles (Scheme S1 in Supporting Information). The results and some redox potentials of relative species are also summarized in Table 4.

Discussion

Mechanism for the Reactions of Ph₃CSNO with T(G)-PPCo^{II} in Benzonitrile. From eq 1, it is evident that the nitrosylation of cobalt in T(G)PPCo^{II} by Ph₃CSNO in benzonitrile solution was completed by NO transfer from Ph₃CSNO to the cobalt atom in T(G)PPCo^{II}. According to the reaction heats listed in Table 1, the reactions of Ph₃CSNO with T(G)PPCo^{II} are all highly exothermic (27.6–31.6 kcal/mol), which indicates that the NO transfer from Ph₃CSNO to T(G)PPCo^{II} in benzonitrile should be easy in the view of the thermodynamics. The main reason could be

Scheme 1. Possible Pathways of NO Transfer from Ph₃CSNO to T(G)PPCo^{II}

$$^a \Delta H(a) = \Delta H_{het}(\text{S}-\text{NO}) \quad (2)$$

$$^b \Delta H(b) = \Delta H_{het}(\text{S}-\text{NO}) - \Delta H_{het}(\text{Co}^{III}-\text{NO}) \quad (3)$$

$$^c \Delta G(c) = -F[E_{red}^{\circ}(\text{Ph}_3\text{CSNO}) - E_{1/2}(\text{TPPCo}^{II})] \quad (4)$$

$$^d \Delta H(d) = \Delta H_{homo}(\text{S}-\text{NO}) - \Delta H_{homo}(\text{Co}^{II}-\text{NO}) \quad (5)$$

$$^e \Delta H(e) = \Delta H_{homo}(\text{S}-\text{NO}) \quad (6)$$

$$^f \Delta H(f) = -\Delta H_{het}(\text{Co}^{III}-\text{NO}) \quad (7)$$

$$^g \Delta H(g) = \Delta H_{homo}(\text{S}-\text{NO}^{\cdot-}) - \Delta H_{homo}(\text{Co}^{III}-\text{NO}) \quad (8)$$

$$^h \Delta H(h) = \Delta H_{het}(\text{S}-\text{NO}^{\cdot-}) - \Delta H_{homo}(\text{Co}^{II}-\text{NO}) - F[E_{1/2}(\text{TPPCo}^{II}) - E_{1/2}(\text{NO}^{0/-})] \quad (9)$$

$$^i \Delta H(i) = -\Delta H_{homo}(\text{Co}^{II}-\text{NO}) \quad (11)$$

$$^j \Delta G(j) = -F[E_{1/2}(\text{TPPCo}^{II}\text{NO}) - E_{ox}^{\circ}(\text{Ph}_3\text{CS}^{\cdot-})] \quad (11)$$

$$^k \Delta H(k) = -1/2 \Delta H_{homo}(\text{Ph}_3\text{CS}-\text{SCPh}_3) \quad (12)$$

the formation of dimer trityldisulfide (Ph₃CS)₂, which releases a great amount of heat (~60.4 kcal/mol). Because of the importance of NO transfer from *S*-nitrosothiols to metal center complexes in vivo, it should be necessary to know the pathway of the NO transfer from Ph₃CSNO to T(G)PPCo^{II}, since this reaction would be a good mimic system of NO transfer in vivo.^{3,17} According to the equation of reaction 1 and the chemical properties of *S*-nitrosothiols and tetraphenylporphyrinatocobalt(II), the possible pathways of NO transfer from Ph₃CSNO to T(G)PPCo^{II} can be proposed as shown in Scheme 1. From Scheme 1, it is clear that there are at least six possible pathways involved in the NO transfer. Since the ability of *S*-nitrosothiols to act as NO, NO⁺, and NO⁻ donors under physiological conditions may be responsible for certain biological activities,²⁴ the six proposed pathways shown in Scheme 1 would all be possible.²⁵ But, which one is the actual pathway of the NO transfer from Ph₃CSNO to T(G)PPCo^{II}? To thoroughly elucidate the most likely mechanisms of the NO transfer and to provide the information necessary to postulate the intrinsi-

- (24) (a) Zhu, X.-Q.; Zhang, J.-Y.; Cheng, J.-P. *Org. Lett.* **2006**, 8 (14), 3065–3067. (b) Stamler, J. S.; Singel, D. J.; Loscalzo, J. *Science* **1992**, 258, 1898–1902 and references therein.
- (25) (a) Arnelle, D. R.; Stamler, J. S. *Arch. Biochem. Biophys.* **1995**, 318, 279. (b) Wang, K.; Zhang, W.; Xian, M.; Hou, Y.-C.; Che, X.-C.; Cheng, J.-P.; Wang, P. G. *Curr. Med. Chem.* **2000**, 7, 821.

Table 5. Energetics of Each Mechanistic Step for the Reactions of Ph₃CSNO with T(G)PPCo^{II} in Benzonitrile Shown in Scheme 1 (kcal/mol)^a

G	ΔH (or ΔG)										
	<i>a</i> ^b	<i>b</i> ^c	<i>c</i> ^d	<i>d</i> ^e	<i>e</i> ^f	<i>f</i> ^g	<i>g</i> ^h	<i>h</i> ⁱ	<i>i</i> ^j	<i>j</i> ^k	<i>k</i> ^l
<i>p</i> -OCH ₃	52.1	28.9	40.1	-1.2	23.4	-23.2	-10.1	-41.2	-24.6	-30.1	-30.2
<i>p</i> -CH ₃	52.1	30.2	41.0	-0.7	23.4	-21.9	-9.8	-41.6	-24.1	-30.9	-30.2
<i>p</i> - <i>i</i> -pr	52.1	30.2	40.7	-0.8	23.4	-21.9	-9.5	-41.4	-24.2	-31.0	-30.2
<i>m</i> -CH ₃	52.1	31.3	41.6	-0.1	23.4	-20.8	-9.2	-41.6	-23.5	-31.5	-30.2
<i>p</i> -H	52.1	31.8	42.2	0.0	23.4	-20.3	-9.4	-42.2	-23.4	-31.8	-30.2
<i>m</i> -OCH ₃	52.1	32.0	42.4	0.1	23.4	-20.1	-9.4	-42.3	-23.3	-32.0	-30.2
<i>p</i> -Cl	52.1	33.6	43.5	0.6	23.4	-18.5	-8.9	-42.9	-22.8	-33.0	-30.2
<i>p</i> -Br	52.1	33.2	43.6	0.1	23.4	-18.9	-9.3	-43.4	-23.3	-33.1	-30.2
<i>m</i> -Cl	52.1	34.0	44.5	0.0	23.4	-18.1	-9.4	-44.4	-23.4	-34.0	-30.2
<i>m</i> -Br	52.1	34.6	44.5	0.6	23.4	-17.5	-8.9	-43.9	-22.8	-34.1	-30.2
<i>m</i> -NO ₂	52.1	37.4	46.1	2.6	23.4	-14.7	-7.7	-43.5	-20.8	-35.1	-30.2
<i>p</i> -NO ₂	52.1	38.0	46.8	2.3	23.4	-14.1	-7.8	-44.4	-21.1	-35.7	-30.2

^a All values were derived in benzonitrile solution at 298 K in kcal/mol. ^{b–l} From eqs 2–12, respectively. The relative heterolytic and homolytic Co–NO bond dissociation energies of T(G)TPPCo^{II}NO and its cation T(G)TPPCo^{III}NO were obtained from the previous paper.^{19a} The relative heterolytic and homolytic S–NO bond dissociation energies of Ph₃CSNO and its radical anion were obtained from the present work (Table 4 and Supporting Information).

cal reaction mechanism, it is very useful and necessary to make detailed thermodynamic analysis on each elementary step for the NO transfer from Ph₃CSNO to T(G)PPCo^{II}NO in benzonitrile. On the basis of Scheme 1, eleven equations (2–12) (where the Faraday constant, F , = 23.06 kcal mol⁻¹ V⁻¹) were developed,²⁶ from which the change of the standard state enthalpy or free energy for each elementary step shown in Scheme 1 can be derived according to the heterolytic and homolytic S–NO, (S–NO)[•], Co^{II}–NO, and Co^{III}–NO bond-dissociation energies of the relative NO-carried compounds and the redox potentials of the relative species, respectively. Detailed thermodynamic values are summarized in Table 5.

The most striking feature of the data in Table 5 is that the energy changes of the initial steps (*a*, *b*, *c*, *d*, and *e*) in the six possible pathways of the NO transfer are all larger than that of the following steps (*f*, *g*, *h*, *i*, *j*, and *k*), which indicates that the initial step of the NO transfer is more difficult in thermodynamics, regardless of the actual pathway of the NO transfer. By comparison of the energy changes of the six initial steps (see columns *a*, *b*, *c*, *d*, and *e* in Table 5), it is clear that the most favorable initial step of the NO transfer is step *d* because, among the six initial steps, only step *d* took place with a decrease or slight increase of the state free energy (-1.2 to 2.3 kcal/mol), which indicates that the pathway of *d*–*k* should be most likely mechanism for reaction 1. Since the free-energy change of step *k* (-30.2 kcal/mol) is much more negative than that of step *d* (-1.2 to 2.3 kcal/mol), it is conceivable that the step *d* could be the rate-determining step. To further verify the mechanism of the reactions of Ph₃CSNO with T(G)TPPCo^{II} (pathway *d*–*k*), the kinetics of the reaction was determined. From

Table 3, it is found that the activation free-energetic scales for the reactions of Ph₃CSNO with T(G)TPPCo^{II} in benzonitrile range from 11.1 kcal/mol when G is *p*-OCH₃ to 12.2 kcal/mol when G is *p*-NO₂. A comparison of the determined activation free energies of the reactions with the corresponding standard-state free-energy changes in the five likely initial reactions (*a*, *b*, *c*, *d*, and *e*) clearly shows that the activation free energies (11.1–12.2 kcal/mol) are much smaller than the corresponding standard-state free energy of the five initial reactions *a* (52.1–52.1 kcal/mol), *b* (28.9–38.0 kcal/mol), *c* (40.1–46.8 kcal/mol), and *e* (23.4–23.4 kcal/mol) but are larger than the corresponding standard state free energy change of the initial reaction *d* (-1.2–2.3 kcal/mol). On the basis of a general *reaction law* which states that the activation free-energy change is always larger than or at least equal to the corresponding standard-state free-energy change for any elemental reaction, it is evident that the initial reactions *a*, *b*, *c*, and *e* should be all ruled out as the initial reaction in the reactions of Ph₃CSNO with T(G)PPCo^{II}; the only remaining reaction, *d*, is suitable for the reaction law, which means that the mechanism of the reactions of Ph₃CSNO with T(G)PPCo^{II} is unambiguously the *d*–*k* pathway. Since the state energy change of the initial step *d* is close to zero, it is easy to conceive that NO transfer from Ph₃CSNO to T(G)PPCo^{II} to form T(G)PPCo^{II}NO and radical Ph₃CS[•] could be reversible. In the reaction of Ph₃CSNO with T(G)PPCo^{II}, the main reason for the rapidly complete transfer of NO from Ph₃CSNO to T(G)PPCo^{II} could be that the formed (triphenylmethyl)sulfanyl radical Ph₃CS[•] in the initial step can rapidly dimerize to generate the disulfide and this releases a great amount of heat, which makes the reaction equilibrium to move to the side of products. The concerned NO transfer mechanism present here would be similar to the direct NO transfer from *S*-nitrosothiols to iron center complex reported by Butler and co-workers,²⁷ suggesting that the NO transfer from the *S*-nitrosothiols to metal center complex act in a direct NO transfer way.

(26) It should be pointed out herein that we used the term free-energy change, ΔG_{et} , to replace the enthalpy change, ΔH_{et} , in eqs 4–6 for the electron-transfer processes. This treatment is valid because the entropies associated with electron transfer are negligible; this has been verified by Arnett's and Bordwell's work. See the following references: (a) Arnett, E. M.; Amarnath, K.; Harvey, N. G.; Cheng, J.-P. *J. Am. Chem. Soc.* **1990**, *112*, 344–355. (b) Bordwell, F. G.; Cheng, J.-P.; Harrelson, J. A., Jr. *J. Am. Chem. Soc.* **1988**, *110*, 1229. (c) Bordwell, F. G.; Bausch, M. J. *J. Am. Chem. Soc.* **1986**, *108*, 1979.

(27) Bulter, A. R.; Elkins-Daukes, S.; Parkin, D.; Williams, D. L. H. *Chem. Commun.* **2001**, 1732.

According to the values of the second-order rate constants in Table 2, it is clear that the range of the rate constants of NO transfer from Ph_3CSNO to $\text{T(G)PPCo}^{\text{II}}$ is from 0.76×10^4 to $4.58 \times 10^4 \text{ M}^{-1} \text{ s}^{-1}$, which is much smaller than the encounter-controlled kinetic criterion, indicating the NO transfer should be reaction-controlled, which is supported by the measured activation free-energy change ($\Delta G^\ddagger = 11.1\text{--}12.2 \text{ kcal/mol}$). From an examination of activation enthalpy and activation entropy of the NO transfer, it is clear that the ΔG^\ddagger is mainly derived from the contribution of activation enthalpy, ΔH^\ddagger , because the activation entropy change of the NO transfer is very small (-3.63 to $-7.75 \text{ cal mol}^{-1} \text{ K}^{-1}$). One key reason for the small activation entropy could be that the length of S–NO bond is long (1.793 \AA),²⁸ much longer than that of N–NO bond about by 0.4 \AA ,²⁹ which results in a larger flexibility of the related groups bound by S–NO bond in the transition state. Since Ph_3CSNO has larger steric hindrance, in general, than the other familiar small molecule S-nitrosothiols, it is possible that for the NO transfers from the general smaller molecule S-nitrosothiols to metal porphyrins, the activation entropies all could be very small, the kinetics of the NO transfer should be mainly controlled by activation enthalpy. According to the definition of enthalpy, it is understandable that the magnitude of activation enthalpy in the NO transfer from Ph_3CSNO to $\text{T(G)PPCo}^{\text{II}}$ is dependent on the breaking of the old S–NO bond and the formation of the new Co–NO bond in the transition state. Generally, the weaker the S–NO bond is or the stronger the $\text{Co}^{\text{II}}\text{--NO}$ bond is, the faster the rate of the NO transfer, which can be well supported by the plot of the $\log k_2$ against the $\text{Co}^{\text{II}}\text{--NO}$ BDEs of $\text{T(G)PPCo}^{\text{II}}\text{NO}$ (Figure S17 in Supporting Information). From this case, a very important prediction can be made that, in the living body, the nitrosylation of metal porphyrin by free NO should be much faster than that by S-nitrosothiols, since for the former reaction, no S–NO bond needs to be broken. In fact, this prediction has been supported by recent paper.^{27,30}

Nature of the Driving Force of NO Transfer from Ph_3CSNO to $\text{T(G)PPCo}^{\text{II}}$. According to the examination above on the mechanism of the reaction of Ph_3CSNO with $\text{T(G)PPCo}^{\text{II}}$, it is evident that the reaction of Ph_3CSNO with $\text{T(G)PPCo}^{\text{II}}$ was initiated by NO transfer. Since NO is a neutral radical and the oxidation number of cobalt atom from $\text{T(G)PPCo}^{\text{II}}$ to $\text{T(G)PPCo}^{\text{II}}\text{NO}$ has no change, an interesting question can be produced about what force made NO transfer from Ph_3CSNO to $\text{T(G)PPCo}^{\text{II}}$ in the rate-determining step. Is it spin–spin coupling affinity like the force making H^\bullet and H^\bullet form H_2 or electrostatic charge attraction like the force making H^+ and H^- form H_2 ? Since NO is a neutral radical

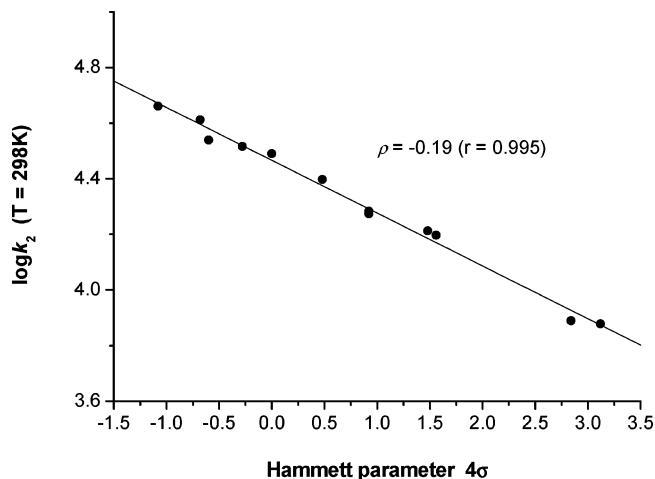


Figure 3. Correlations of $\log k_2$ (at 298 K) vs Hammett parameter 4σ for the reaction of Ph_3CSNO with $\text{T(G)PPCo}^{\text{II}}$ in benzonitrile.

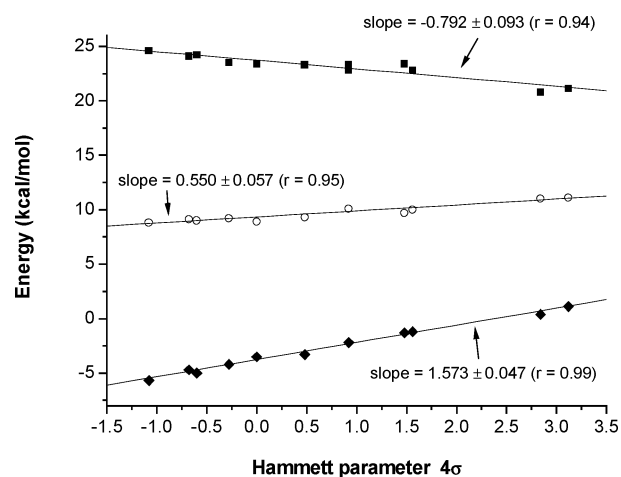


Figure 4. Hammett plots of the ΔH^\ddagger for the reaction of Ph_3CSNO with $\text{T(G)PPCo}^{\text{II}}$ (○), $\Delta H_{\text{homo}}(\text{Co}^{\text{II}}\text{--NO})$ (■), and ΔG_{ET} for the electron transfer from $\text{T(G)PPCo}^{\text{II}}$ to NO^+ (◆) vs 4σ .

and $\text{T(G)PPCo}^{\text{II}}$ also is a neutral radical,³¹ it is easy to believe that the spin–spin coupling affinity could be the dominant driving force pushing NO from Ph_3CSNO to $\text{T(G)PPCo}^{\text{II}}$. Is that true? To elucidate the nature of the driving force, the spin-delocalization effect and polar effect of the substituents G in $\text{T(G)PPCo}^{\text{II}}$ on the reaction rate constants were examined. The results show that no good linear relationship of $\log k_2$ with the spin-delocalization parameter, $4\sigma_{\text{jj}}^*$,³² was observed for the porphyrin substituents (Figure S14 in Supporting Information) meaning that the rate of NO transfer from Ph_3CSNO to $\text{T(G)PPCo}^{\text{II}}$ is insensitive to the spin-delocalization effect of the substituents G, that is, the spin–spin coupling effect could not be the main driving force of the NO transfer. For the plot of $\log k_2$ with Hammett polar parameter 4σ (Figure 3), an excellent straight line with line slope of -0.19 was observed, indicating that the electrostatic dipole charge attraction would be the main driving force to make NO transfer from Ph_3CSNO to $\text{T(G)PPCo}^{\text{II}}$. In fact, from the good binary-correlation plot of $\log k_2$ against 0.76σ

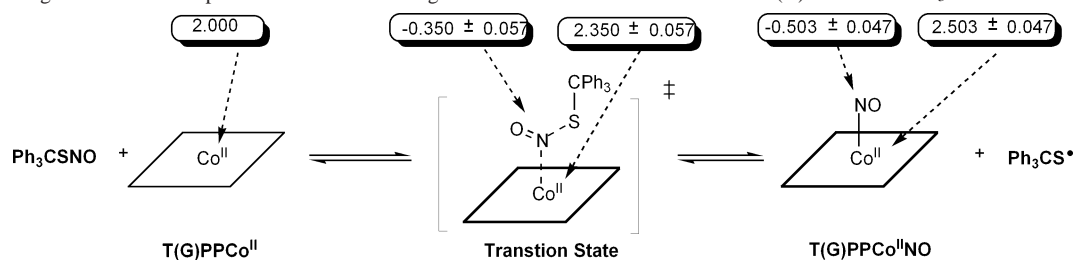
(28) Arulsamy, N.; Bohle, D. S.; Butt, J. A.; Irvine, G. J.; Jordan, P. A.; Sagan, E. *J. Am. Chem. Soc.* **1999**, *121*, 7115–7123.

(29) (a) Ohwada, T.; Miura, M.; Tanaka, H.; Sakamoto, S.; Yamaguchi, K.; Ikeda, H.; Inagaki, S. *J. Am. Chem. Soc.* **2001**, *123*, 10164. (b) Bartberger, M. D.; Houk, K. N.; Powell, S. C.; Mannion, J. D.; Lo, K. Y.; Stamler, J. S.; Toone, E. J. *J. Am. Chem. Soc.* **2000**, *122*, 5889.

(30) Franke, A.; Stochel, G.; Suzuki, N.; Higuchi, T.; Okuzono, K.; Eldik, R. *J. Am. Chem. Soc.* **2005**, *127*, 5360–5375.

(31) Kamachi, M.; Shibasaka, M.; Kajiwar, A.; Mori, W.; Kishita, M. *Bull. Chem. Soc. Jpn.* **1989**, *62*, 2465–2473.

(32) (a) Jiang, X.-K.; Ji, G.-Z. *J. Org. Chem.* **1992**, *57*, 6051. (b) Jiang, X.-K. *Acc. Chem. Res.* **1997**, *30*, 283.

Scheme 2. Charge-Distribution Map on the Rate-Determining Transition State for the Reaction of T(G)PPCo^{II} with Ph₃CSNO in Benzonitrile^a

^a The porphyrin ring is shown as a square.

+ 0.07 σ_{jj} (Figure S15 in Supporting Information), it is clear that the effect of spin–spin interaction on the driving force is very small. To further support the nature of the driving force, the dependence of the reaction rate on the oxidation potentials of the NO acceptors [T(G)PPCo^{II}] was examined (Figure S16 in Supporting Information), the results exhibit an excellent straight line with a slope of -2.75 ($r = 0.98$), which means that the driving force of the NO transfer should be significantly dependent on the electron-donating ability (Lewis basicity) of T(G)PPCo^{II}. Since the value of the line slope is negative (-2.75), it is possible that T(G)PPCo^{II} is a Lewis bases, NO in Ph₃CSNO is a Lewis acid, and the combination of them in reaction *d* was essentially driven by the interaction of Lewis acid and Lewis bases. In fact, from Table 1, it is immediately evident that the oxidation potential of T(G)PPCo^{II}NO is larger than that of the corresponding T(G)PPCo^{II} by 0.259–0.306 V, indicating that the electrochemical cobalt center in T(G)PPCo^{II}NO is a poorer electron donor than that in the corresponding T(G)PPCo^{II}.

Evaluation of the Effective Charge Distribution on the Co Atom in NO Transfer Process. To elucidate the Lewis acid nature of NO group in T(G)PPCo^{II}NO and examine the charge transfer during the NO transfer from Ph₃CSNO to T(G)PPCo^{II}, the effective charge distribution on the cobalt atom in the reactant T(G)PPCo^{II}, the transition-state, and the product T(G)PPCo^{II}NO needs to be estimated. Since Hammett linear free-energy relationship analysis can provide a very efficient access to estimate the effective charge distribution,^{33,34} the plots of the activation enthalpy (ΔH^\ddagger) for the reaction of Ph₃CSNO with T(G)PPCo^{II}, the Co^{II}–NO BDEs in T(G)PPCo^{II}NO, and the free-energy changes (ΔG_{ET}) for electron transfer from T(G)PPCo^{II} to NO⁺ against the Hammett substituent constant 4σ were made, and three excellent straight lines with slopes of 0.550 ± 0.057 , -0.792 ± 0.093 , and 1.573 ± 0.047 ³⁵ were obtained, respectively (Figure 4), which means that Hammett linear free-energy relationship holds in the three reaction processes. According

to the nature of the Hammett substituent effect, it is possible that the sign of the line slope values reflects increase or decrease of the effective charge on the cobalt atom and that the magnitude of the line slope values is a measure of the effective charge change at the cobalt atom during the corresponding reaction processes.^{19a} Since the positive line slope of 1.573 ± 0.047 for the plot of ΔG_{ET} versus 4σ is equivalent to the oxidation number increase of the cobalt atom from T(G)PPCo^{II} to T(G)PPCo^{III}, it is clear that the positive line slope of 0.550 ± 0.057 for ΔH^\ddagger would also be equivalent to the oxidation number increase of the cobalt atom from T(G)PPCo^{II} to the transition state, but the negative line slope of -0.792 ± 0.093 for $\Delta H_{\text{homo}}(\text{Co}^{\text{II}}\text{--NO})$ would be equivalent to the oxidation number decrease of the cobalt atom from T(G)PPCo^{II}NO to T(G)PPCo^{II}. If we define the oxidation numbers of the cobalt atom in T(G)PPCo^{II} and T(G)PPCo^{III} as +2 and +3, respectively, it can be deduced that the effective charge on the cobalt atom would be 2.350 ± 0.057 and 2.503 ± 0.047 units in the transition state and in T(G)PPCo^{II}NO, respectively. The details of the effective charge change on the cobalt atom during NO transfer from Ph₃CSNO to T(G)PPCo^{II} is shown in Scheme 2. From Scheme 2, it is clear that although the NO went from Ph₃CSNO to T(G)PPCo^{II} without heterolytic S–NO bond dissociation in Ph₃CSNO, the effective positive charge on the cobalt atom always kept increasing from the reactant T(G)PPCo^{II} (+2.000) to the transition state (+2.350) and finally to the product T(G)PPCo^{II}NO (+2.503). The concerted NO transfer from Ph₃CSNO to T(G)PPCo^{II} with the release of Ph₃CS• radical was actually performed by the initial negative charge (-0.350) transfer from T(G)PPCo^{II} to Ph₃CSNO to form the transition state, followed by homolytic S–NO bond dissociation of Ph₃CSNO with a further negative charge (-0.153) transfer from T(G)PPCo^{II} to the NO group to form the final product T(G)PPCo^{II}NO. Since the negative charge on nitrosyl group are increased as the increase of the positive charge on the cobalt atom from the reactant T(G)PPCo^{II} (+2.000) to the transition state (+2.350) finally to the product, it is evident that the nature of the driving force of the NO transfer in reaction step *d* is indeed electrostatic attraction of positive charge and negative charge. In addition, if one compares the charge distribution in the transition state and in the product T(G)PPCo^{II}NO, one finds that the charge change on the cobalt atom from the reactants T(G)PPCo^{II} to the transition state is 0.350 unit, which is larger than the

- (33) (a) Page M.; Williams A. *Organic and Bio-organic Mechanism*; Addison Wesley Longman: Boston, 1997; Chapter 3, pp. 52–79. (b) Williams A. *Acc. Chem. Res.* **1984**, *17*, 425. (c) Williams A. *Acc. Chem. Res.* **1989**, *22*, 387. (d) Williams A. *Adv. Phys. Org. Chem.* **1991**, *27*, 1. (e) Williams A. *J. Am. Chem. Soc.* **1985**, *107*, 6335. (34) (a) Zhu, X.-Q.; Cao, L.; Liu, Y.; Yang, Y.; Lu, J.-Y.; Wang, J.-S.; Cheng, J.-P. *Chem.—Eur. J.* **2003**, *9*, 3937. (b) Zhu, X.-Q.; Li, H.-R.; Li, Q.; Ai, T.; Lu, J.-Y.; Yang, Y.; Cheng, J.-P. *Chem.—Eur. J.* **2003**, *9*, 871. (35) The line slope of the plot of ΔG_{ET} against 4σ is 1.573 ± 0.047 rather than the 1.618 ± 0.07 value in the previous literature.^{18a} The value of 1.618 in the previous paper is wrong because of our careless mistake. Herein, a special apology is given to the readers.

half of the change from the reactants to the product T(G)-PPCo^{II}NO (0.503/2 = 0.252 unit), suggesting that the transition state of the nitrosylation of T(G)PPCo^{II} by Ph₃-CSNO would be productlike (Scheme 2), similar to the case for the nitrosations of alanine, glycine, valine, and anilines by nitrosating agents such as ONCl, ONBr, ONSCN, etc.³⁶

Conclusions

In this work, the thermodynamics and kinetics of NO transfer from Ph₃CSNO to T(G)PPCo^{II} in benzonitrile were investigated, and the reaction mechanism of the NO transfer was elucidated according to the related thermodynamic and kinetic parameters, for which the determination of the heterolytic and homolytic S–NO bond dissociation energies of Ph₃CSNO and its radical anion in benzonitrile were also made. The following conclusions can be made. (1) The reaction of Ph₃CSNO with T(G)PPCo^{II} to yield T(G)PPCo^{II}-NO and the dimer of (Ph₃CS)₂ is highly exothermic, which indicates that the reactions are much favorable in thermodynamics; the main reason is that the formed (triphenylmethyl)sulfanyl radical Ph₃CS• can dimerize to release large amounts of heat. (2) NO transfer from Ph₃CSNO to T(G)-PPCo^{II} is a concerted process of the homolytic S–NO bond dissociation and the formation of the Co–NO bond; the rate of the NO transfer was controlled by activation enthalpy, which is obviously different from the previous thought that the NO transfer from *S*-nitrosothiol to metal porphyrin could be initiated by NO⁺ transfer.²⁴ (3) In the reaction of Ph₃-CSNO with T(G)PPCo^{II}, NO in the *S*-nitrosothiol is a typical Lewis acid and T(G)PPCo^{II} is a typical Lewis base; the main driving force of the NO transfer is electrostatic dipole charge attraction rather than a spin–spin coupling interaction. (4) The effective charge distribution on the cobalt atom in the porphyrin ring at the various stages, the reactant [T(G)-PPCo^{II}], the transition-state, and the product [T(G)PPCo^{II}-NO], was estimated to show that the cobalt atom carries relative effective positive charges of 2.000 in the reactant [T(G)PPCo^{II}], 2.350 in the transition state, and 2.503 in the product [T(G)PPCo^{II}NO], respectively, which indicates that the concerted NO transfer from Ph₃CSNO to T(G)PPCo^{II} was practically performed by the initial negative charge transfer of –0.350 from T(G)PPCo^{II} to Ph₃CSNO to form the transition state and an additional negative charge transfer (–0.153) from T(G)PPCo^{II} to NO.

Experimental Section

Materials. Compounds T(G)PPCo^{II} (*G* = *p*-OCH₃, *p*-CH₃, *p*-i-Pr, *m*-CH₃, *H*, *m*-OCH₃, *p*-Cl, *p*-Br, *m*-Cl, *m*-Br, *m*-NO₂, *p*-NO₂) were synthesized as previously described.^{19a,20} Ph₃CSNO³⁷ and NO⁺ClO₄^{–38} were prepared according to the published procedures and used as fresh reagents (see Supporting Information). All solvents

were treated according to standard procedure, and the benzonitrile solution was carefully degassed before each experiment.

Spectrophotometric Kinetic Measurements. The kinetic determination of the reactions of T(G)PPCo^{II} with Ph₃CSNO were performed on an Applied Photophysics SX.18MV-R stopped-flow spectrophotometer under anaerobic operation, which was thermostated (±0.1 °C) by circulating water, by rapid mixing of the T(G)-PPCo^{II} with an excess of Ph₃CSNO (15 ~70 fold) using single mixing mode. The kinetic traces were recorded on an Acorn computer and analyzed by Pro-K Global analysis/simulation software or translated to PC for further analysis. The pseudo-first-order rate constants (*k*_{obs}) can be calculated by fitting the data with the equation of $\text{abs} = P_1 \exp(-k_{\text{obs}}t) + P_2$, which was integrated in the Pro-K Global analysis/simulation software or Origin Software (Figure S6 in the Supporting Information). The application of the Guggenheim method gives the same value of the rate constants *k*_{obs}. The second-order-rate constants were derived from the slopes of the plots of versus the concentration of Ph₃-CSNO (Figure S7 in the Supporting Information). In each case, it was confirmed that the rate constants derived from five to seven independent measurements agreed within an experimental error of ±5%.

Isothermal Titration Calorimeter Experiments. Isothermal titration calorimeter experiments were performed in benzonitrile solution at 298 K on a CSC 4200 isothermal titration calorimeter. Prior to use, the instrument was calibrated against an internal heat pulse. Data points were collected every 2 s. For the reaction of Ph₃CS[–] with NO⁺, the reaction heat was determined following nine automatic injections from a 250 μL injection syringe containing 0.85 mM NO⁺ (NO⁺ClO₄[–]) into the reaction cell (1.00 mL) (containing 0.47 mM Ph₃CS[–]). Injection volumes (10 μL) were delivered at 0.5 s intervals with 400 s between each set of injections. The reaction heat was obtained by area integration of each peak except the first one. For the reaction of Ph₃CSNO with T(G)PPCo^{II}, the reaction heat was determined following eight automatic injections from a 250 μL injection syringe containing 1.37 mM T(G)-PPCo^{II} into the reaction cell (1.00 mL) (containing 1.54 mM Ph₃CSNO). Injection volumes (10 μL) were delivered at 0.5 s intervals with 400 s between every two injections. The reaction heat was obtained by area integration of each peak except the first one.

Measurement of Redox Potentials. All electrochemical experiments were carried out by CV (sweep rate, 100 mV/s) using a BAS-100B electrochemical apparatus in dry benzonitrile solution under an argon atmosphere at 298 K as described previously.^{19a} *n*-Bu₄-NPF₆ (0.1 M) was employed as the supporting electrolyte. A standard three-electrode cell consists of a glassy carbon disk as working electrode, a platinum wire as counter electrode, and 0.1 M AgNO₃/Ag (in 0.1 M Bu₄NPF₆-PhCN) as the reference electrode. All sample solutions were 1.5 mM. The ferrocenium/ferrocene redox couple (Fc^{+/0}) was taken as the internal standard. The reproducibility of the potentials was usually ≤5 mV for ionic species and ≤10 mV for neutral species.

Acknowledgment. Financial support from the Ministry of Science and Technology of China (Grant 2004CB719905), the National Natural Science Foundation of China (Grants 20272027, 20332020, 20472038, and 20672060), Ministry of Education of China (Grant 20020055004), and Natural Science Fund of Tianjin (Grant 033804311) is gratefully acknowledged.

Supporting Information Available: Experimental details, estimation of the heterolytic and homolytic S–NO bond-dissociation

- (36) (a) da Silva, G.; Kennedy, E. M.; Dlugogorski, B. Z. *J. Am. Chem. Soc.* **2005**, *127*, 3664–3665. (b) da Silva, G.; Kennedy, E. M.; Dlugogorski, B. Z. *Ind. Eng. Chem. Res.* **2004**, *43*, 2296–2301.
(37) Arulsamy, N.; Bohle, D. S.; Butt, J. A.; Irvine, G. J.; Jordan, P. A.; Sagan, E. *J. Am. Chem. Soc.* **1999**, *121*, 7115–7123.
(38) Markowitz, M. M.; Ricci, J. E.; Goldman, R. J.; Winternitz, P. F. *J. Am. Chem. Soc.* **1957**, *99*, 3659.

energies of Ph_3CSNO , the corresponding IR and UV–vis spectra for the reactants and products, the data fitting of k_{obs} and the derivation of k_2 , the Arrhenius plot of $\ln k_2$ versus $1/T$, as well as the Eyring plot of $\ln (k_2/T)$ versus $1/T$ for the NO transfer reaction, plots of $\log k_2$ (at 298 K) versus (i) spin-delocalization parameter $4\sigma_{\text{II}}^*$, (ii) σ and σ_{II}^* , (iii) oxidation potentials of $\text{T(G)PPCo}^{\text{II}}$, and

(iv) $\text{Co}^{\text{II}}\text{--NO}$ BDEs of $\text{T(G)PPCo}^{\text{II}}\text{NO}$ for the reactions of $\text{T(G)PPCo}^{\text{II}}$ with Ph_3CSNO . This material is available free of charge via the Internet at <http://pubs.acs.org>.

IC061427V